Nanotechnology

Hyperthermic triggers for drug delivery platforms

To cite this article before publication: Lilian C. Alarcon Segovia *et al* 2023 *Nanotechnology* in press https://doi.org/10.1088/1361-6528/ad0480

IOP Publishing Journal Title
Journal **XX** (XXXX) XXXXXX https://doi.org/XXXX/XXXX

Hyperthermic triggers for drug delivery platforms

Lilian C Alarcón-Segovia[1,2], Maria R Morel[3], Jorge I Daza-Agudelo[3], Juan C Ilardo[3] and Ignacio Rintoul[3]*

[1] Instituto de Matemática Aplicada del Litoral. Universidad Nacional del Litoral and Consejo Nacional de Investigaciones Científicas y Técnicas, Argentina.
[2] Universidad María Auxiliadora, Asunción, Paraguay.
[3] Instituto de Desarrollo Tecnológico para la Industria Química. Universidad Nacional del Litoral and Consejo Nacional de Investigaciones Científicas y Técnicas, Argentina.

Email of corresponding author: irintoul@santafe-conicet.gov.ar

Received xxxxxx
Accepted for publication xxxxxx
Published xxxxxx

Abstract

Electromagnetic fields can penetrate aqueous media in a homogeneous and instantaneous way, without physical contact, independently of its temperature, pressure, agitation degree and without modifying their chemical compositions nor heat and mass transfer conditions. In addition, superparamagnetic biomaterials can interact with electromagnetic fields by absorbing electromagnetic energy and transforming it in localized heat with further diffusion to surrounding media. This paper is devoted to the exploration of the potential use of hyperthermic effects resulting from the interaction between externally applied electromagnetic fields and superparamagnetic nanoparticles as a trigger for controlled drug release in soft tissue simulating materials. Gelatin based soft tissue simulating materials were prepared and doped with superparamagnetic nanoparticles. The materials were irradiated with externally applied electromagnetic fields. The effects on temperature and diffusion of a drug model in water and phosphate buffer were investigated. Significant hyperthermic effects were observed. The temperature of the soft tissue simulating material resulted increased from 35°C to 45°C at 2.5 °C/min. Moreover, the release of an entrapped model drug reached 89%. The intensity of the hyperthermic effects was found to have a strong dependency on the concentration of superparamagnetic nanoparticles and the power and the pulse frequency of the electromagnetic field.

Keywords: biomaterials, microwaves, magnetic field

1. Introduction

The control of the kinetics of drug release is one of the most challenging fields in pharmaceutics and drug delivery research [1,2]. Several drug release triggers such as pH, ionic strength, temperature, diffusion and degradation processes have been largely investigated with the purpose of controlling the kinetics of drug delivery mechanisms [3-7].

Moreover, photodynamic effects on nanoparticles specifically designed for targeted cancer treatment are also investigated. Electromagnetic fields within the light range are capable of developing interesting interactions on cancer cells internalized nano particles resulting in remarkable photomediated cytotoxicity and apoptosis [8]

The smart application of drug release triggers may result in drug delivery systems with controlled or programmed release patterns. These delivery systems are designed and synthesized to release drugs according to previously well defined kinetics [9].

The exploration of nanomaterials with action mechanisms relying on interactions with externally applied

IOP Publishing Journal Title
Journal **XX** (XXXX) XXXXXX https://doi.org/XXXX/XXXX

electromagnetic energy is emerging as a novel trigger alternative for drug release systems [10,11].

Electromagnetic energy can be easily generated by alternating magnetic fields and propagates very efficiently through aqueous media [12]. In particular, externally applied electromagnetic fields can penetrate biological tissues in a homogeneous and instantaneous manner [13,14]. Moreover, the action of these fields can be carried out without physical contact and independently of the physical, chemical and biological internal condition of the body. Moreover, externally applied radiofrequency may act selectively over superparamagnetic biocompatible materials tailored designed as drug release triggers.

The synthesis of controlled drug release platforms resulting from the incorporation of biocompatible nanomaterials to biocompatible polymers seems to be technically easy and very effective to study electromagnetic interactions. In particular, superparamagnetic nanoparticles (SPMNPs) can be used as triggers for localized delivery of drugs using electromagnetic mechanisms [15-17]. SPMNPs have the capability to absorb and transform externally applied electromagnetic energy into thermal energy. The transformation occurs by the internal dipole rotation of Néel relaxation mechanism and by the physical Brownian relaxation mechanism. The strengths of these mechanisms are intrinsically related to the size, shape, composition, and concentration of the SPMNPs, the viscosity, composition and density among other characteristics of their surrounding medium and the characteristics of the externally applied electromagnetic field [18,19].

The heat generated by the interaction between electromagnetic fields and SPMNPs are currently used in hyperthermia treatments and in different combinations of hyperthermia with chemotherapy treatments to increase the effect of therapies in tumor killing, in reducing the amount of administrated drugs and in minimizing non-desired effects [20,21].

Drugs and heat diffusion may adopt different models according to the shape, size and material characteristics of the device and the dosage form of the drug into the device [22,23].

This work raises the hypothesis of using the hyperthermic effect enhanced by SPMNPs as a novel trigger method for the release of drugs entrapped in hydrogel matrices. The specific research objectives of this study are the elucidation of the features of electromagnetic field interactions with SPMNPs through a gelatin based soft tissue simulating materials and the quantification of the hyperthermic effects in terms of concentration of SPMNPs and the frequency and intensity of externally applied alternating electromagnetic fields commonly used for kinesiology treatments.

2. Experimental parts

2.1 Materials

SPMNPs were synthesized using ferric chloride hexahydrate (Biopack, Argentina), ferrous chloride tetrahydrate (Biopack, Argentina), ammonium hydroxide 28% w/w (Anedra, Argentina), N_2 ultrapure grade 4.5 (Indura, Argentine), water of Millipore quality, resistivity of 18.2 MΩ and density δw = 0.99704 g/cm3 and absolute methanol (Cicarelli, Argentina) as iron sources, pH adjustment, reaction medium and washing solvent, respectively.

Type I B gelatin with Bloom 180-260 (AN-MAX FG3 PB Liner, Argentina), glycerol (Cicarelli, Argentina) and crystal violet (CV) (Sigma-Aldrich, Germany) were used as substrate polymer, plasticizer and drug model. A Biocellular Regenerator medical device (CEC Electronica, Argentina) was used to stimulate the system with different radiofrequency patterns. The Biocellular Regenerator is a medical device commonly used for kinesiology treatments. An infrared digital thermometer (Model VA6520, Shanghai Yi Hua V&A Instiment Co., China) was used for measuring the temperature of the system in an instant and non-contact manner. Phosphate buffer (SBF) (Sigma Aldrich, USA) was used to prepare testing media.

2.2 Synthesis of SPMNPs

SPMNPs were prepared by a co-precipitation method [24,25]. Briefly, 6.22 g of ferrous chloride and 2.29 g of ferric chloride, in 2:1 Fe3+/Fe2+ ratio, were dissolved in 50 ml of water. The solution was mixed at 1000 rpm of stirring speed and 70 °C of temperature. The system was kept under N_2 atmosphere to avoid side reactions. Then, 25.6 mL of ammonium hydroxide were added drop wise. Afterwards, the solution was left to evolve maintaining the same reaction conditions during 60 minutes. After that, dark precipitate was precipitated and recovered by magnetic sedimentation using strong neodymium magnets. The recovered material was firstly washed with deionized water and secondly with methanol to remove all Cl- ions and residual ammonium hydroxide. The final product was vacuum dried during 45 minutes and then stored until use in a hermetically sealed container [24,25].

2.3 Characterization of SPMNPs

The purity, crystalline phase and size of the ordered domains of the obtained product was characterized using an X-ray diffractometer (X-RD), (X-ray Diffractometer Model XD-D1 Shimadzu, Japan). The X-RD operated with a Cu-Kα X-ray source with wavelength λ = 1.54Å. The mean crystallite size was calculated using the Debye–Scherrer equation according to a reference method [24]. The morphology, the average particle size and particle size

IOP Publishing Journal Title
Journal **XX** (XXXX) XXXXXX https://doi.org/XXXX/XXXX

distribution were determined using a high-resolution transmission electron microscope (TEM), (JEOL 100 CX II, Japan) operating at 100 kV and magnifications of 270000x – 450000x. The software of the microscope permitted to discriminate, count, measure and perform statistical analysis of the particles. The superparamagnetic behaviour was determined by a SQUID system (MPMS SQUID magnetometer, Quantum Design, USA) at T = 27 °C.

2.4 Preparation of hydrogel nanocomposite (nHG) materials

nHG materials were prepared according a modified sol-gel method [26]. These materials were designed to develop mechanical properties mimicking those of skin and connective tissues [26]. First, a stock solution was prepared by dissolving 12.5 g of gelatin and 6.5 g of glycerol in 376 g of water. Second, the stock solution was divided in 5 parts of 79 g each. Third, different amounts of SPMNPs were added in to the solutions to obtain the following weigh percentages of SPMNPs respect to the amount of gelatin: 0%, 5%, 10%, 15% and 20%. The suspensions were stirred during 15 minutes and subsequently poured in petri dishes. Fourth, the suspensions were left to gel and evaporate water until constant weight to form the nHG materials. Gelation process was carried out during 48hs in a chamber set at 40°C and 50% of relative humidity. It is important to place the petri dishes perfectly horizontal to ensure homogeneous thickness of the resulting membranes. Gelation occurs by tropocolagenic linking of gelatin molecules [26].

Finally, a small spot of CV was deposited in the center of the nHG loaded petri dishes.

2.5 Diffusion of mass and heat through RF stimulated nHG

The nHG samples were irradiated with RF using a Biocellular Regenerator. The nHG samples were exposed to RF of different intensities and during different pulse frequencies. The temperatures in the nHG materials were recorded using an infrared digital thermometer. The time derivatives of nHG temperature were calculated as the slope of the measured temperatures vs. time (dT/dt). The diffusion of CV was measured as a function of time in distilled water and SBF solution by UV-Visible spectroscopy.

3. Results and discussion

3.1 X-RD diffraction

Figure 1 shows the X-RD pattern of the product obtained by the co-precipitation method. The correspondence to the Miller indices (hkl) of crystal lattice are also indicated in the X-RD pattern. The position and intensity of peaks are well correlated with those reported for magnetite and maghemite in the literature [27-29]. It is important to note that magnetite and maghemite present the same X-RD pattern. The X-RD pattern reports the absence of any other type of iron oxide. The average crystallite size resulted 9.7 nm.

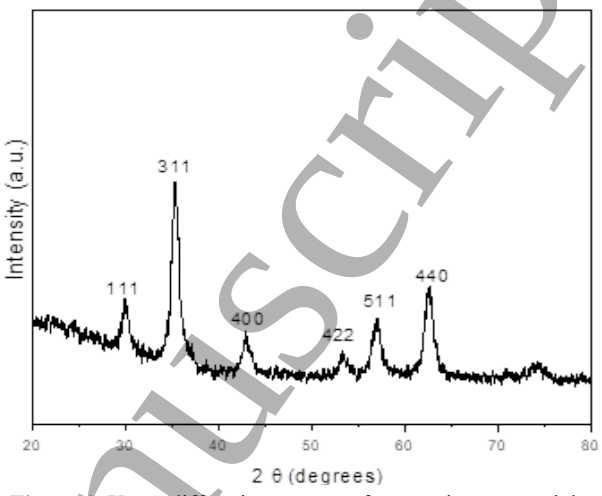

Figure 1. X-ray diffraction pattern of magnetic nanoparticles.

3.2 Morphology and particle size

Figure 2 shows a TEM image of the product obtained by co-precipitation method. Clearly, the precipitated particles tend to form magnetic aggregates. The particles occur in near spherical shape with normal size distribution. The mean particle size ± 2 standard deviations resulted: 10.3 nm ± 1.1 nm. The mean particle size resulted slightly higher than the average size of ordered domains (cristallite size). Hence, the obtained product may be considered to be composed of quasi-monocrystalline nanoparticles [24,30].

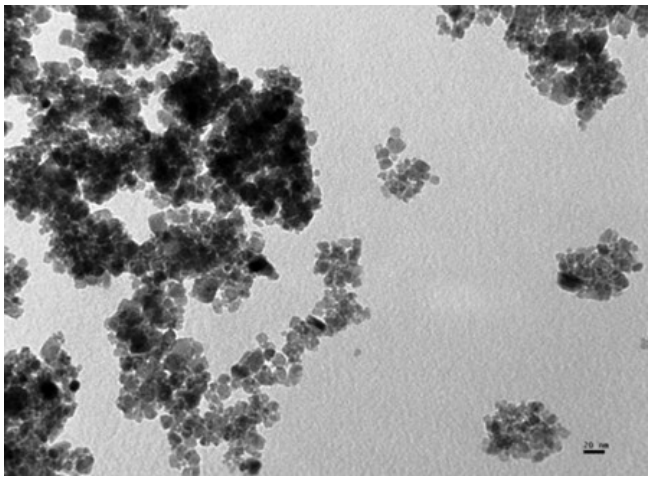

Figure 2. TEM image of magnetite nanoparticles.

3.3 Magnetic properties

Figure 3 shows the magnetic behaviour at 27°C of the product obtained by the co-precipitation method. The plot exhibits typical superparamagnetic behaviour due the

IOP Publishing Journal Title
Journal **XX** (XXXX) XXXXXX https://doi.org/XXXX/XXXX

absence of hysteresis loops, remanence and coercivity [31]. The saturation magnetization resulted 92 emu/g.

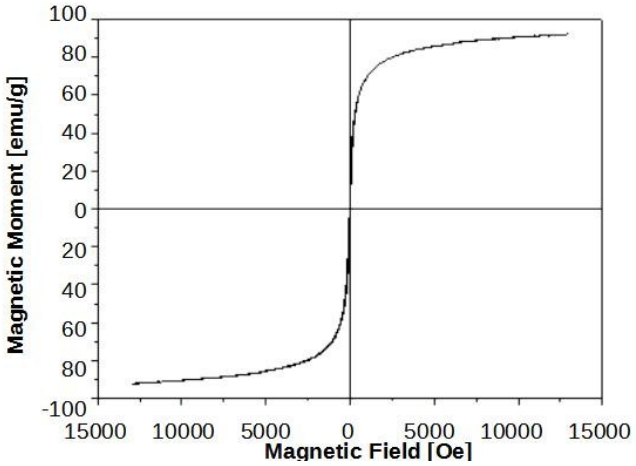

Figure 3. SQUID measurement of co-precipitated nanoparticles.

3.4 Superparamagnetic iron oxide nanostructures

Iron oxide magnetic nanoparticles produced by chemical synthesis are usually composed of both, magnetite and maghemite phases [32]. Magnetite-maghemite mixtures are reported to develop superparamagnetic property at nanoscale [32-34]. The X-RD, TEM and SQUID characterizations of the product obtained by the co-precipitation method are consistent with the results reported in the literature for superparamagnetic nano magnetite-maghemite [32-34]. The X-RD and TEM analysis revealed a clear spinel iron oxide nanostructure of about 10 nm of particle size and composed of nothing more than magnetite-maghemite phases. In conclusion, the obtained product of the co-precipitation method is consistent with results reported for quasi-monocrystalline near spherical superparamagnetic nanoparticles of 10.3 nm ± 1.1 nm of diameter and 92 emu/g of saturation magnetization.

3.5 Heat diffusion through nHG stimulated with radiofrequency (RF)

Figure 4 presents the time evolution of the temperature measured at the contact point between the RF electrode and the nHG material as a function of SPMNP concentration. The RF stimulation was set at constant 50 Hz of pulsated power and applying different power levels. It shows clear evidence of the hyperthermic effect of SPMNPs over the irradiated nHG material. Hydrogels with SPMNPs increased their temperature significantly faster than hydrogels without SPMNPs when they were stimulated by RF. Absorption of electromagnetic energy by SPMNPs with further heat transformation and diffusion to the aqueous surrounding medium is a generally accepted mechanism to explain this behaviour. Higher concentration of SPMNPs in the nHG promoted faster increase of temperature of the nHG. The temperature was also increased by the increment of the RF power.

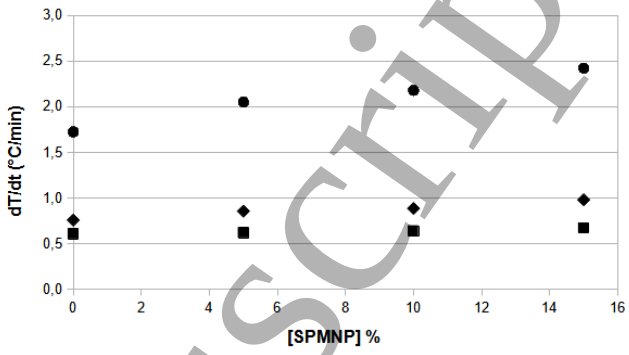

Figure 4. Time evolution of temperature in nHG materials under RF stimulation at 50 Hz of pulsated power at different SPMNP concentrations and power levels: 12 W (■); 20 W (♦) and 28 W (●).

Figure 5 presents the time evolution of temperature in the contact point between the RF electrode the nHG material. Here, the RF stimulation was set at different pulse frequencies and using a constant power of 20 W. The variation of the temperature increase with the pulse frequency of RF is clearly visible. The increase of frequency, in terms of pulses per second, changed the amount of energy provided by the RF to the system. Between each pulse, the nHG could dissipate thermal energy. An increase of RF frequency reduced the dissipation time and increased the temperature of the irradiated nHG material. The highest temperatures were reached when the nHG material was continuously irradiated.

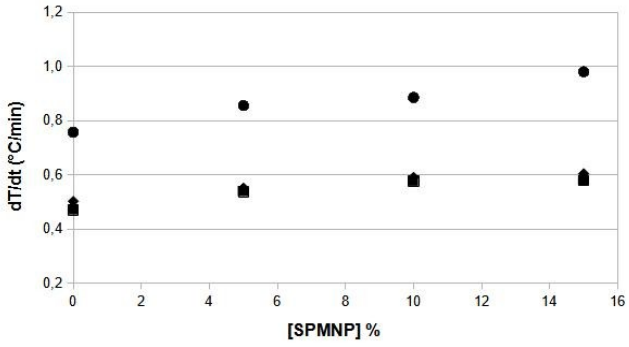

Figure 5. Time evolution of temperature in nHG materials under RF stimulation of 20 W at different SPMNP concentrations and pulse frequencies: 5 Hz (■); 20 Hz (♦) and 50 Hz (●).

3.6 Hyperthermic trigger for drug release

Figure 6 presents the release profiles of CV in nHG material loaded with 5% of SPMNPs. The release conditions were set at 35 °C and 45 °C, in water and SBF media. Table 1 presents quantitative values.

IOP Publishing Journal Title
Journal **XX** (XXXX) XXXXXX https://doi.org/XXXX/XXXX

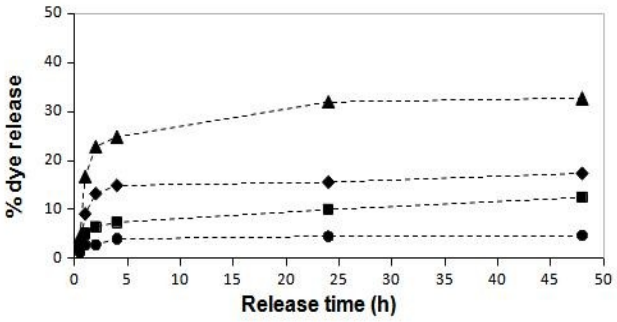

Figure 6. CV release in nHG material with 5% of SPMNPs under RF stimulation. Water temperature: 35 °C (●), 45 °C (■); SBF temperature: 35 °C (♦), 45 °C (▲).

The kinetic release of CV resulted faster in SBF medium than in pure water for both temperatures. The initial release rate in SBF resulted almost five times higher than in water at 45 °C and seven times higher at 35 °C. Additionally, the initial release rate of CV resulted higher at 45°C than at 35°C. The initial release rate at 45 °C resulted almost double than at 35 °C in SBF and almost three times higher in water.

The amount of CV released in water resulted 3 times higher at 45°C than at 35 °C. In SBF medium the increment was approximately doubled. Such a differences may be explained by the competing presence of ions in the medium with limiting effects in the release of CV.

Table 1. Initial release rate and maximum released amount of CV in each media for nHG material loaded with 5% of SPMNPs.

Temp. °C	Medium	Initial Release Rate (%/h)	Max CV Released (%)
35	Water	0.96	4.69
35	SBF	6.86	17.35
45	Water	2.54	12.43
45	SBF	11.42	32.74

4. Conclusions

The presence of SPMNPs in soft-tissue mimicking hydrogels permits to capture externally applied electromagnetic energy and to transform it into thermal energy. The time accumulation of thermal energy increases the temperature of the surrounding soft-tissue mimicking hydrogels and activate the release of a model drug by increasing the release rate and the total amount of released drug. This hyperthermic effect resulted enhanced by increasing the concentration of SPMNPs and the power and the pulse frequency of the externally applied RF.

The hyperthermic effect was demonstrated to work as trigger for the release of a model drug model. This result confirms the potential of hyperthermic trigger mechanism to control the kinetics of drug releasing systems using externally applied RF stimuli.

Future research directions may include in-vitro and ex-vivo hyperthermic studies of controlled drug delivery, the determination of hyperthermic effects on diffusion coefficients of drugs and studies about radiofrecuency penetration in tissues of different densities and water contents.

Conflicts of interest: There are no conflicts to declare.

Acknowledgements: The authors thank the Universidad Nacional del Litoral (UNL), Consejo Nacional de Investigaciones Científicas y Técnicas (CONICET) and the Fondo para la Investigación Científica y Tecnológica (FONCYT) for the financial support. Grants: PICT 2015 1785 and PIP 1118.

References

[1] Milano F, Masi A, Madaghiele M, Sannino A, Salvatore L and Gallo N 2023 *Pharmaceutics* **15** 1499
[2] Brewster P, Mohammad-Ishraq-Bari S, Walker G and Werfel T 2023 *Advanced Drug Delivery Reviews* **197** 114824
[3] Zhuo S, Zhang F, Yu J, Zhang X, Yang G and Liu X 2020 *Molecules* **25** 1
[4] Asare-Addo K, Conway B, Larhrib H, Levina M, Rajabi-Siahboomi A, Tetteh J, Boateng J and Nokhodchi A 2013 *Colloids Surfaces B Biointerfaces* **111** 384
[5] Verkhovskii R, Ivanov A, Lengert E, Tulyakova K, Shilyagina N and Ermakov A 2023 *Pharmaceutics* **15** 1566
[6] Yahya I, Ahmed L, Omara A, Eltayeb M, Atif R and Eldeen T 2019 *International Journal of Research and Science Innovation* **6** 287
[7] Joiner J, Prasher A, Young I, Kim J, Shrivastava R, Maturavongsadit P and Benhabbour S 2022 *Pharmaceutics* **14** 615
[8] Bartelmess J, Milcovich G, Maffeis V, d'Amora M, Bertozzi SM and Giordani S. 2020 *Frontiers in Chemistry* **8** 573211
[9] Wang X, Li C, Wang Y, Chen H, Zhang X, Luo C, Zhou W, Li L, Teng L, Yu H and Wang J 2022 *Acta Pharmaceutica Sinica B* **12** 4098
[10] Xu W, Xie X, Wu H, Wang X, Cai J, Xu Z and Shiju E 2022 *View* **3** 20220029
[11] Tian H, Zhang T, Qin S, Huang Z, Zhou L, Shi J, Nice E, Xie N, Huang C and Shen Z 2022 *Journal of Hematology and Oncology* **15** 132
[12] Rintoul I 2017 *Processes* **5** 15
[13] Fortin J, Gazeau F and Wilhelm C 2008 *European Biophysics Journal* **37** 223
[14] Matsumura S, Hlil A, Lepiller C, Gaudet J, Guay D, Shi Z, Holdcroft S and Hay A 2008 *Journal Polymer Science. Part A Polymer Chemistry* **46** 7207
[15] Reczynska K, Marszalek M, Zarzycki A, Reczynski W, Kornaus K, Pamula E, Chrzanowski W 2020 *Nanomaterials* **10** 1076

[16] Ferjaoui Z, Jamal-Al-Dine E, Kulmukhamedova A, Bezdetnaya L, Soon-Chang C, Schneider R, Mutelet F, Mertz D, Begin-Colin S, Quiles F, Gaffet E and Alem H 2019 *ACS Applied Materials & Interfaces* **11** 30610
[17] Ansari S, Hempel N, Asad S, Svedlindh P, Bergstrom C, Lobmann K and Teleki A 2022 *ACS Applied Materials & Interfaces* **14** 21978
[18] Tabatabaei S, Tabatabaei M, Girouard H and Martel S 2016 *International Journal of Hyperthermia* **32** 657
[19] Torres-Lugo M and Rinaldi C 2013 *Nanomedicine* **8** 1689
[20] Hervault A and Thanh N 2014 *Nanoscale* **6** 11553
[21] Rodzinski A, Guduru R, Liang P, Hadjikhani A, Stewart T, Stimphil E, Runowicz C, Cote R, Altman N, Datar R and Khizroev S 2016 *Scientific Reports* **6** 1
[22] Siepmann J and Siepmann F 2008 *International Journal of Pharmaceutics* **364** 328
[23] Higuchi T 1961 *Journal of Pharmaceutical Sciences* **50** 874
[24] Alarcon-Segovia L, Daza-Agudelo J, Glisoni R, Acha C, De-Zan M and Rintoul I 2020 *Nanotechnology* **31** 185604
[25] Alarcon-Segovia L, Bandodkar A, Rogers J and Rintoul I 2021 *Nanotechnology* **32** 37510
[26] Alarcón-Segovia L, Daza-Agudelo J and Rintoul I 2021 *Polymers* **13** 1991
[27] Swanson E, Mc-Murdie H, Morris H and Evans E 1967 Standard x-ray diffraction powder patterns. Washington. National Bureau of Standards Monograph 25 Section 5
[28] Reichmann H and Jacobsen S 2004 *American Mineralogist* **89** 1061
[29] Mahdavi M, Bin-Ahmad M, Haron M, Namvar F, Nadi B, Ab-Rahman M and Amin J 2013 *Molecules* **18** 7533
[30] Li Q, Kartikowati C, Horie S, Ogi T, Iwaki T and Okuyama K 2017 *Scientific Reports* **7** 1
[31] Zhao X, Shi Y, Wang T, Cai Y and Jiang G 2008 *Journal of Chromatography A* **1188** 140
[32] Dehsari H, Ksenofontov V, Moller A, Jakob G and Asadi K 2018 *Journal of Physical Chemistry C* **122** 28292
[33] Tadic M, Kralj S, Jagodic M, Hanzel D and Makovec D. 2014 *Applied Surface Science* **322** 255
[34] Tadic M, Lazovic J, Panjan M and Kralj S 2022 *Ceramics International* **48** 16015